Probing the origin of gamma-ray emission towards the W41 region with H.E.S.S. and *Fermi* LAT

JÉRÉMIE MÉHAULT[1*], FABIO ACERO[1], JOHANN COHEN-TANUGI[1], FABRICE FEINSTEIN[1], MARIE-HÉLÈNE GRONDIN[3], MARIANNE LEMOINE-GOUMARD[2], MATTHIEU RENAUD[1]
FOR THE H.E.S.S. AND FERMI-LAT COLLABORATIONS
[1]*Laboratoire Univers et Particules de Montpellier - Montpellier - France*
[2]*Centre d'Études Nucléaires de Bordeaux Gradignan - Bordeaux - France*
[3]*Institut für Astronomie und Astrophysik Tübingen - Tübingen - Germany*
[*]*jeremie.mehault@lupm.in2p3.fr*
DOI: 10.7529/ICRC2011/V07/0900

Abstract: Extended very high energy gamma-ray emission from the direction of the W41 supernova remnant (G23.3-0.3) was first discovered by the H.E.S.S. Cherenkov telescopes and confirmed by MAGIC. However, the origin of this emission is still in debate. Different scenarios such as pulsar wind nebula or interaction with a giant molecular cloud (GMC) were proposed. Furthermore, a central compact object was detected in X-rays by XMM-*Newton* and recently by *Chandra*. This object is surrounded by a diffuse X-ray emission, supposed to be a dust halo or a pulsar wind nebula, could be the pulsar associated with W41.
The discovery of high energy γ-ray emission towards W41 with *Fermi* LAT opens the possibility to study jointly with H.E.S.S. this region over seven decades in energy, helping us to unveil the origin of the γ-ray emission towards the W41 region.

Keywords: gamma rays - galactic source - SNR: G23.3-0.3 - ISM: giant molecular cloud - PWN: CXOU J183434.9084443

1 Introduction

The High Energy Stereoscopy System (H.E.S.S.) collaboration reported the detection of a bright, extended (intrinsic width $\sigma = 0.2^{o}$) very high energy (VHE) γ-ray source HESS J1834–087 [3] spatially coincident with the supernova remnant (SNR) G23.3-0.3 (aka W41) thanks to a 7 hour live-time observation. The distance of the remnant has been estimated between 3.9 and 4.5 kpc by HI [10] and CO absorption [13]. The associated cloud used for the distance estimation has a radial velocity in the local standard of rest of 77 km/s. An age between 6.10^4 and 2.10^5 yrs has been proposed, depending on the expansion model [18]. In X-rays, XMM-*Newton* [16] and *Chandra* [15] detected a pulsar candidate at the centre of the remnant, but no pulsation were found. The putative pulsar is coincident with a compact non-thermal X-ray nebula which could be a dust halo or a pulsar wind nebula (PWN). PWN and interacting SNR with molecular cloud have been proposed to explain the VHE γ-ray emission [5].
Additional observation time has been obtained with H.E.S.S. telescopes which allow us to perform joint morphological and spectral analyses with *Fermi* LAT data.

2 H.E.S.S. observations and analysis

H.E.S.S. is an array of four identical 13-m diameter imaging atmospheric Cherenkov telescopes (IACTs) located in the Khomas Highland of Namibia ($23°16'18''$ S $16°30'00''$ E) at an altitude of 1800 m above the sea level. Each of these telescopes covers a large field-of-view (FoV) of 5^{o} diameter. Due to its large FoV and geographic situation, H.E.S.S. is ideally suited for studies of extended sources and Galactic plane survey.
The dataset used for this work correspond to 50 hours live-time which represent a significant improvement in comparison with the 7 hours in the discovery paper. The data has been analysed with the Xeff reconstruction method [7] which has a better sensitivity than more common techniques. The studied source is very bright $S \sim 23\,\sigma$ within $0.3°$ radius around the pulsar candidate position. A second independent analysis chain was used to cross-check the results, including independent calibration of pixel amplitudes and identification of dead pixels in the IACTs cameras, leading to compatible results.

2.1 Morphological analysis

Figure 1 presents the excess map smoothed to the H.E.S.S. point spread function ($r_{68\%} = 0.062°$). Radio contours

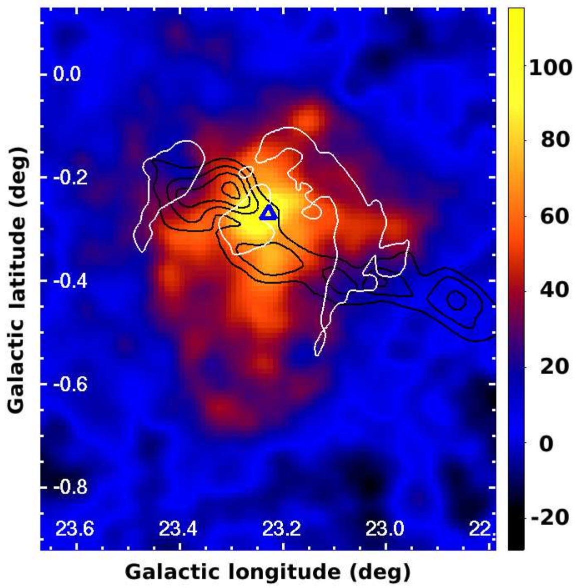

Figure 1: Excess map of the SNR W41 FoV smoothed with the point spread function (PSF) of the H.E.S.S. experiment ($r_{68\%} = 0.062°$). Black contours represents the ^{13}CO data from the GRS integrated around W41's velocity (between 74 km/s and 82 km/s), whereas the white contours shows the NRAO radio data at 20 cm. The pulsar candidate XMMU J183435.3–084443 is represented by a blue triangle.

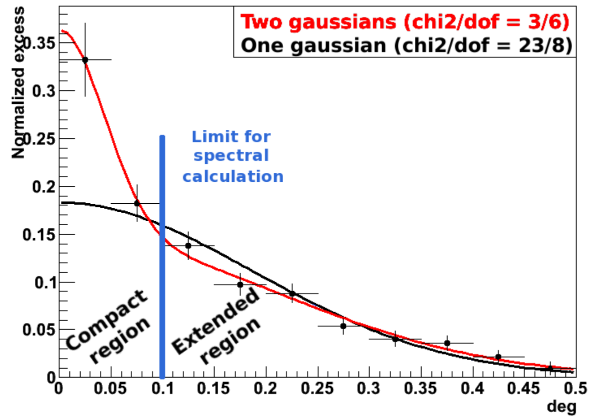

Figure 2: Radial profile of normalised excesses centred on the pulsar candidate position. The best-fit model is composed by two gaussians (red line) compared to the single gaussian (black line).

(white) from the shell, cloud density (black) traced by ^{13}CO from the Galactic Ring Survey (GRS) [12], and new pulsar candidate (triangle) are shown as well.

The best-fit position of the excess ($l = 23.24° \pm 0.01°_{stat}, b = -0.27° \pm 0.01°_{stat}$) is compatible with the pulsar candidate position ($l = 23.235°, b = -0.269°$) which has been chosen to perform the radial profile in figure 2. The latter shows that a double components function (red) fit better the data ($\chi^2 = 3/6$) than a single gaussian ($\chi^2 = 26/8$). The central peak and the extended emission are each modeled by a gaussian. Their intrinsic sizes are respectively: $r_{int_{cent}} = (0.04 \pm 0.01)$ deg and $r_{int_{ext}} = (0.20 \pm 0.01)$ deg. No correlation between γ-ray and cloud morphologies is observed.

2.2 Spectral analysis

In order to test for spectral variations in the compact and annular regions, two distinct spectral extraction regions were used. In figure 2, the blue line at $r_{int} = 0.1°$ defines the limit between central and annnular regions. The annular boundary $r_{ann} = 0.3°$ has been chosen to select significant excess ($S > 4\sigma$) on Gaussian-smoothed excess map ($\sigma = 0.11°$). The *multiple reflected regions technique* has been used to evaluate the background in the FoV. The central emission is analyzed within a circular region of radius $0.1°$. Its spectrum is better fitted by an exponential cut off power law ($\chi^2 = 13/15$ dof) than a pure power law ($\chi^2 = 24/16$ dof):

$$\frac{\mathrm{d}N}{\mathrm{d}E} = \Phi_0(E_0) \times \left(\frac{E}{E_0}\right)^{-\Gamma} \times \exp\left(\frac{-E}{E_{cut}}\right) \qquad (1)$$

with $\Phi_0(E_0) = (3.52 \pm 0.64_{\rm stat}) \times 10^{-8}$ m^{-2}s^{-1}TeV^{-1}, $E_0 = 0.653$ TeV, the spectral index $\Gamma = 1.6 \pm 0.3_{\rm stat} \pm 0.1_{\rm sys}$ and the energy cut $E_{cut} = 1.9 \pm 0.8$ TeV.

The spectra extracted inside the annular region presents a pure power law spectrum ($\chi^2 = 40/20$ dof) with a normalization constant of $\Phi_0(E_0) = (10.47 \pm 0.63_{\rm stat}) \times 10^{-8}$ m^{-2}s^{-1}TeV^{-1}, $E_0 = 0.580$ TeV, and a photon index of $\Gamma = 2.6 \pm 0.1_{\rm stat} \pm 0.1_{\rm sys}$.

3 *Fermi* LAT observations and analysis

The Large Area Telescope (LAT), launched in June 2008 onboard the *Fermi* observatory, observes the entire γ-ray sky every 3 hours, thanks to its wide field-of-view (FoV) of 2.4 sr. For a detailed description of the instrument, see [6]. The data used in this work have been acquired between 4 August 2008 and 10 June 2010, which is more than used in the 1FGL catalogue [1]. Only γ-ray events coming from zenith angles smaller than $100°$ have been selected in order to reduce the Earth albedo contribution. Events have been selected from 1 GeV to 100 GeV in the *P6_DIFFUSE* class. Such cut selection is motivated by point spread function better than $1.0°$ (for 68% containment) at 1 GeV, and the difficulties to model the associated diffuse emission.

Figure 3 shows the TS map with superimposed TS *Fermi* LAT contours from 40 increasing by step of 40 obtained with Pointlike analysis. The source is very bright with $\mathrm{TS}_{max} = 153$. The best morphological fit of the high energy (HE) γ-ray excess is obtained with an extended gaussian model which is statisticaly better than a point-like source ($\mathrm{TS}_{ext} = 47$). The intrisic size is $\sigma =$

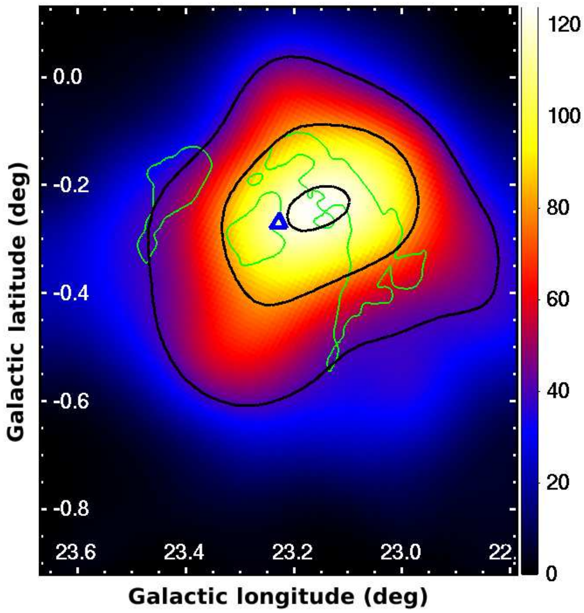

Figure 3: TS map with TS contours 40, 80, 120 from *Fermi* analysis using PointLike. Only events above 1 GeV were used.

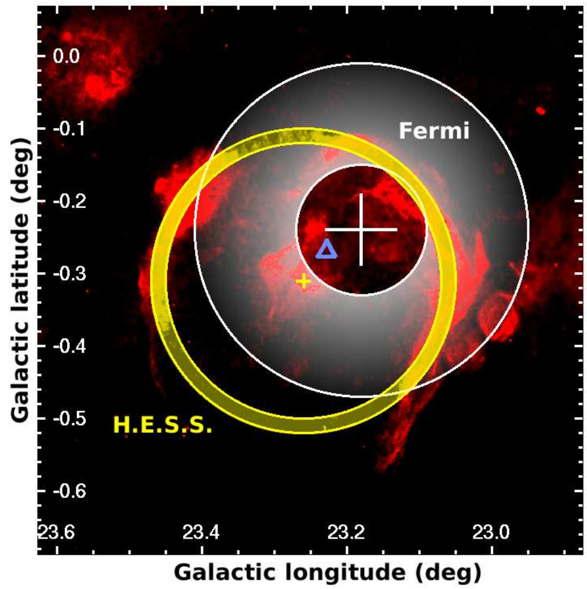

Figure 4: Radio map from VLA with superimposed positions and intrinsic size in white and yellow respectively for *Fermi* LAT and H.E.S.S. sources. The crosses size informs the position error, whereas the ring's thickness represents the extensions errors.

$(0.16 \pm 0.07)^\circ$ and the best-fit position ($l = 23.18^\circ \pm 0.05^\circ$, $b = -0.24^\circ \pm 0.05^\circ$) is compatible with SNR W41.

The best-fits results demonstrate that GeV and TeV extended components have compatible intrinsic sizes. Moreover, figure 4 presents the comparison of best-fits positions (crosses) and extensions (the rings represents the statistical uncertainties) from *Fermi* LAT (white) and H.E.S.S. (yellow) analysis. Their position are both compatible with W41.

The spectra associated to the *Fermi* source can be modeled as an integrated power law function:

$$\frac{\mathrm{d}N}{\mathrm{d}E} = I_0 \frac{(\alpha + 1)E^\alpha}{E_{max}^{\alpha+1} - E_{min}^{\alpha+1}} \tag{2}$$

with $I_0 = 1.2 \pm 0.1 \times 10^{-8}$ cm^{-2}s^{-1} the integrated flux between $E_{min} = 1$ GeV and $E_{max} = 100$ GeV and $\alpha = 2.1 \pm 0.1$ the spectral index.

4 Discussion

4.1 GeV - TeV morphology comparison

GeV and TeV extended emission are compatible in terms of position and intrisic extension. Figure 5 shows the spectral energy distibution (SED) from GeV to TeV energies. Because the spectra of both extended emissions joint smoothly, the same mechanism can be at the origin of these emissions. The TeV central emission (blue butterfly) can not be observed by *Fermi* LAT because its flux is to low.

4.2 Shell-type morphology scenario

The origin of the γ-ray emission from the SNR shell is unlikely because of the morphology. The emission is not a shell-like morphology as RX J1713–3946 at VHE [4] or W44 at HE [2]. On the contrary, the VHE radial profile shows that the main emission comes from the centre of the SNR.

4.3 SNR-MC interaction

Four interacting SNRs are known with associated γ-ray emission from GeV to TeV energies, namely IC443, W28, W44, W51. Their spectra presents two parts, below the energy cut (around 1 - 3 GeV) the power law spectra follows an index of 1.9 or 2.1, while above the break the index is between 2.6 and 3.1.

The possibility for W41 to be in interaction with the associated GMC has been suggested [5]. From the best-fit position performed with H.E.S.S., it is clear that the TeV emission is not coincident with the ^{13}CO peak extracted from GRS data [12]: the angular distance between each is around 0.11°. Moreover, the TeV morphology is not compatible with the cloud morphology.

Looking at the SED, the indexes found for the extended emissions are respectively 2.1 ± 0.1 and 2.6 ± 0.1 at GeV and TeV energies. This shape is comparable to interacting SNRs's, but requires a rather high energy cut off (~ 100 GeV) compared to those observed.

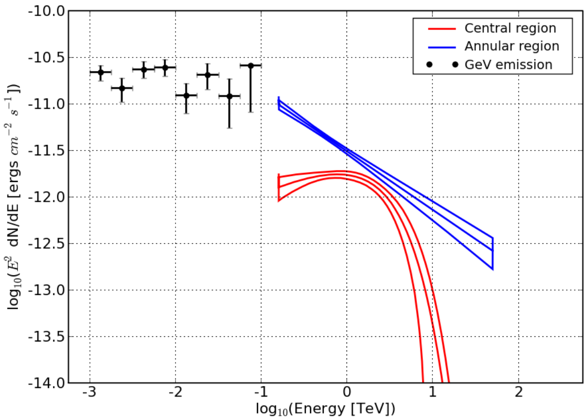

Figure 5: Spectral energy distribution from GeV to TeV energies. The TeV spectra are the 1σ confidence regions of the fits.

4.4 Pulsar wind nebula candidate

Because of the putative X-ray nebula surrounding the pulsar candidate at the center of the remnant, the PWN scenario has been tested. From PWNs observed in X-ray and γ-ray, a correlation between luminosities ratio (L_γ/L_X) and the characteristic age τ_c of the pulsar at the origin of the emission seems to exist [14]. In our case, the range allowed on τ_c is estimated based on the data dispersions. We assumed the whole (central + annular) VHE γ-ray emission coming from the source and estimated $L_\gamma \simeq 2.4 \times 10^{34}$ erg/s, whereas *Chandra* observations provided $L_X \simeq 4.1 \times 10^{33}$ erg/s. We found $\tau_c \in [5.10^3; 8.10^4]$ yr comparing to the W41's estimated age (between 6.10^4 and 2.10^5 yr), then the PWN scenario can't be rejected. In addition, based on X-ray observations, the spin down luminosity estimated from PWN modelisation $\dot{E} \in [10^{36} - 10^{37}]$ erg/s (see [15]) is compatible with values of other TeV PWN.

5 Conclusion

The detailed study of *Fermi* LAT HE γ-ray excess from SNR W41 revealed an extended emission. At VHE, the latest H.E.S.S. data exhibit a two-component morphology. *Fermi* LAT analysis results in a significant extension of the GeV emission which has a compatible intrinsic size with the TeV extended component. Their positions are both in coincidence with SNR W41. The shape of the GeV to TeV spectra is compatible with those of the interacting SNRs even if an energy break around 100 GeV is required. Unfortunately, the CO-γ-ray morphological aspect does not support this scenario.

The central position of the pulsar candidate suggests its association with SNR W41. The surrounding X-ray diffuse emission detected by *Chandra* could be explained by a PWN, the VHE central component is spatially compatible with it. The ratio luminosities between γ- and X-rays of the whole TeV emission and the estimated $\dot{E}$ of the pulsar candidate are in the range of what have been observed in other TeV sources powered by pulsars.

Acknowledgement
The support of the Namibian authorities and of the University of Namibia in facilitating the construction and operation of H.E.S.S. is gratefully acknowledged, as is the support by the German Ministry for Education and Research (BMBF), the Max Planck Society, the French Ministry for Research, the CNRS-IN2P3 and the Astroparticle Interdisciplinary Programme of the CNRS, the U.K. Science and Technology Facilities Council (STFC), the IPNP of the Charles University, the Polish Ministry of Science and Higher Education, the South African Department of Science and Technology and National Research Foundation, and by the University of Namibia. We appreciate the excellent work of the technical support staff in Berlin, Durham, Hamburg, Heidelberg, Palaiseau, Paris, Saclay, and in Namibia in the construction and operation of the equipment.
The *Fermi* LAT Collaboration acknowledges support from a number of agencies and institutes for both development and the operation of the LAT as well as scientific data analysis. These include NASA and DOE in the United States, CEA/Irfu and IN2P3/CNRS in France, ASI and INFN in Italy, MEXT, KEK and JAXA in Japan, and the K. A. Wallenberg Foundation, the Swedish Research Council and the National Space Board in the Sweden. Additional support from INAF in Italy and CNES in France for science analysis during the opreations phase is also gratefully acknowledged.

References

[1] Abdo, A. A. et al. 2009, ApJS, **183**: 46.
[2] Abdo, A. A. et al. 2010, Science, **327**: 1103.
[3] Aharonian, F. et al. 2006, A&A, **636**: 777.
[4] Aharonian, F. et al. 2004, Nature, **432**: 75.
[5] Albert, J. et al. 2006, ApJ, **643**: L53.
[6] Atwood, W. B., et al. 2009, ApJ, **697**: 1071
[7] Dubois, F. et al. 2009, Astropart. Physic., **32**: 73.
[8] Fazio, G. G. et al. 2004, ApJS, **154**: 10.
[9] Gaensler, B. M. & Johnson, S. 1995, MNRAS, **275**: L73.
[10] Gordon, C. P. et al. 1976, ApJ, **203**: 593.
[11] Helfand, D. J. et al. 2006, AJ, **131**: 2525.
[12] Jackson, J. M. et al. 2006, ApJS, **163**: 145.
[13] Leahy, D. A. & Tian, W. W. 2008, AJ, **135**: 167.
[14] Mattana, F. et al. 2009, ApJ, **694**: 12.
[15] Misanovic, Z. et al. 2011, arXiv/1101.1342
[16] Mukherjee, R. et al. 2009, ApJ, **691**: 1707.
[17] Rieke, G. H. et al. 2004, ApJS, **154**: 25.
[18] Tian, W. W. et al. 2007, ApJ, **657**: L25.